# High-Gain Wideband Filtering Quasi-Yagi Antenna Based on High-Order Mode of SSPPs

Daotong Li<sup>®</sup>, Senior Member, IEEE, Ning Pan<sup>®</sup>, Hao Wang<sup>®</sup>, Jiang Dong, Graduate Student Member, IEEE, Qi Jiang<sup>®</sup>, Ying Liu<sup>®</sup>, Naoki Shinohara<sup>®</sup>, Fellow, IEEE, and Qiang Chen<sup>®</sup>, Senior Member, IEEE

Abstract—A high-gain wideband filtering antenna based on the high-order mode of spoof surface plasmon polaritons (SSPPs) is proposed. Excellent filtering characteristics with six radiation nulls (RNs) are obtained from the first high-order mode (mode 1) of SSPP feedline. A novel ground-free single-unit transition structure (GFSTS) is introduced to facilitate smooth momentum transition and impedance matching between the SSPP feedline and driven dipole. The inherent bandpass response of the highorder mode of SSPPs enables the proposed filtering antenna to operate without additional filtering structures, thus avoiding insertion loss and achieving a simplified design. The low-loss transmission characteristic of the SSPP feedline, along with the elimination of insertion loss from external filtering components, enhances the radiation efficiency of the quasi-Yagi antenna. To validate the feasibility of the proposed antenna, a prototype is fabricated and measured. Good endfire characteristics are obtained with a bandwidth of 3.76-6.3 GHz (50.5%), a peak gain of 9.98 dBi, and the out-of-band suppression larger than 18.8 dB. The measured results are in good agreement with the

Index Terms—Filtering antenna, high-order mode, quasi-Yagi antenna, spoof surface plasmon polaritons (SSPPs).

#### I. Introduction

WITH the rapid advancement of wireless communication technologies, antennas—being a crucial component of communication systems—are evolving toward greater integration and multifunctionality. Filtering antennas can effectively suppress interference signals and reduce mutual coupling between antenna elements operating at different frequencies, thereby enabling the design of more compact systems. The filtering quasi-Yagi antenna has been widely studied due to its low profile, low cost, endfire radiation pattern, and high directivity [1], [2], [3].

Received 14 December 2024; revised 25 May 2025; accepted 18 June 2025. Date of publication 3 July 2025; date of current version 14 October 2025. This work was supported by the Chongqing Natural Science Foundation under Grant CSTB2024NSCQ-MSX1038 and Grant CSTB2024NSCQ-MSX1217. (Corresponding author: Daotong Li.)

Daotong Li is with the School of Microelectronics and Communication Engineering, Chongqing University, Chongqing 400044, China, and also with the Research Institute for Sustainable Humanosphere, Kyoto University, Kyoto 606-8501, Japan (e-mail: dli@cqu.edu.cn).

Ning Pan, Hao Wang, Jiang Dong, Qi Jiang, and Ying Liu are with the School of Microelectronics and Communication Engineering, Chongqing University, Chongqing 400044, China.

Naoki Shinohara is with the Research Institute for Sustainable Humanosphere, Kyoto University, Kyoto 606-8501, Japan.

Qiang Chen is with the Department of Communications Engineering, Tohoku University, Sendai 980-8579, Japan (e-mail: qiang.chen.a5@tohoku.ac.jp).

Digital Object Identifier 10.1109/TAP.2025.3583825

Filtering antennas can be broadly classified into three categories based on design approaches. The first method involves integrating a filter into the antenna's feeding network, either by adding a complete filter [1], [4] or specific structures [5], [6], [7] to generate transmission zeros for filtering functionality. This approach allows independent antenna and filter design but leads to low integration and high insertion loss, reducing radiation efficiency. An alternative approach modifies the radiator to suppress or cancel the radiating currents, thereby creating radiation nulls (RNs) on either side of the passband using techniques such as parasitic elements [8], slots [9], [10], or shorting pins [11], [12]. These antennas achieve higher integration levels, with RNs minimally affecting operational band performance. However, their complex structures make design optimization challenging. Additionally, certain design schemes only generate RNs in specific directions [10], [12], while nonnegligible gain remains in other directions, resulting in insufficient interference rejection. Finally, filter synthesis integrates the radiator as the filter's final resonator, enabling radiating capabilities [13], [14], [15]. Antennas designed with this approach excel in integration, bandwidth, and selectivity. However, the insertion loss of the filter is inevitable, thereby reducing the overall radiation efficiency. In summary, most reported filtering antennas feature a broadside radiation pattern, with their filtering capabilities often accompanied by transmission losses that reduce gain. Reducing these losses introduced is a crucial approach to improving the gain of filtering antennas.

Spoof surface plasmon polaritons (SSPPs) are subwavelength periodic structures that support electromagnetic wave modes analogous to surface plasmon polaritons at lower frequencies. SSPPs offer high field confinement, low loss, and conformability, making them ideal for recent microwave applications like power dividers [16], filters [17], [18], and antennas [19], [20].

The single-mode transmission characteristics of the highorder mode in SSPPs can be achieved using a simple and compact transition structure, facilitating the design of various BPFs with excellent in-band transmission performance [21], [22]. In addition, exciting multiple order modes of SSPPs can generate multiple passbands, and eliminating the stopbands between these passbands to achieve broadband performance is feasible. For example, in [23], a multiband antenna is realized by designing units that support multiple high-order modes of SSPPs. The subsequent introduction of I-shaped resonators eliminated the stopbands between the individual passbands, resulting in an ultrawideband endfire antenna. Based on the fundamental mode of SSPPs, some filtering antennas [20], [24] and endfire antennas [19], [25] have been reported. Antennas [20], [24] and endfire antennas [19], [25] have been reported. The filtering performance in these designs is mainly achieved through via holes and ring resonators [24] or by utilizing the low-pass characteristics of the fundamental mode of SSPPs in combination with other techniques [20]. The introduction of SSPPs is primarily aimed at reducing transmission loss to enhance gain. However, existing filtering antennas that incorporate SSPPs technology still rely on additional filtering structures to achieve their filtering functionality. As a result, these antennas suffer from nonnegligible losses and exhibit relatively complex structures as well as enormous sizes. To the best of the authors' knowledge, filtering antennas solely relying on SSPPs have not yet been reported.

In this article, a high-gain wideband filtering quasi-Yagi antenna is implemented relying on the single-mode transmission and low-loss characteristics of SSPPs. The feedline supporting the high-order mode of SSPPs not only provides filtering characteristics independently, avoiding additional lossy filtering structures, but also enhances the antenna gain due to SSPPs' inherent low-loss properties. The proposed novel ground-free single-unit transition structure (GFSTS), achieving significant size reduction compared to traditional tapered transitions, facilitates smooth momentum transition between the high-order mode of SSPPs and the driven dipole. The SSPP feedline and balun generate six RNs, endowing the antenna with excellent frequency selectivity and strong stopband suppression. A prototype of the proposed antenna achieves a wide -10-dB impedance bandwidth from 3.76 to 6.3 GHz and a peak gain of 9.98 dBi.

The arrangement of this article is as follows. Section II presents the configuration of the proposed antenna. Section III presents the mechanism of metallic strips feedline supporting high-order mode of SSPPs of the proposed high-gain wideband filtering quasi-Yagi antenna. Section IV gives the fabrication and experimental results of the proposed high-gain wideband filtering quasi-Yagi antenna based on high-order mode of SSPPs. Finally, the conclusion is drawn in Section V.

#### II. ANTENNA CONFIGURATION

As shown in Fig. 1, the overall structure of the antenna consists of four main components: the balun, high-order mode of SSPP feedline, GFSTS, and the radiation element. Fig. 2 shows the configuration of the proposed planar printed high-gain wideband filtering quasi-Yagi antenna based on high-order mode SSPPs, in which the SSPPs components are enlarged for clarity. Only one layer of Rogers5880 dielectric substrate with a permittivity of 2.2, a loss tangent  $\tan\delta$  of 0.0009, and a thickness of 0.787 mm is used in this design. As shown in Fig. 2(a), the feedline supporting high-order mode of SSPPs is used for both filtering characteristics and high-gain performance. The GFSTS crucially ensures a smooth momentum transition. Additionally, a director parasitic element and a pair of reflector elements on the top layer further enhance the gain and improve the radiation pattern. The microstrip feed

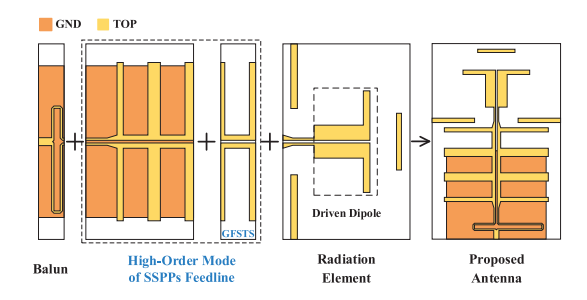


Fig. 1. Structural diagram of the proposed filtering antenna.

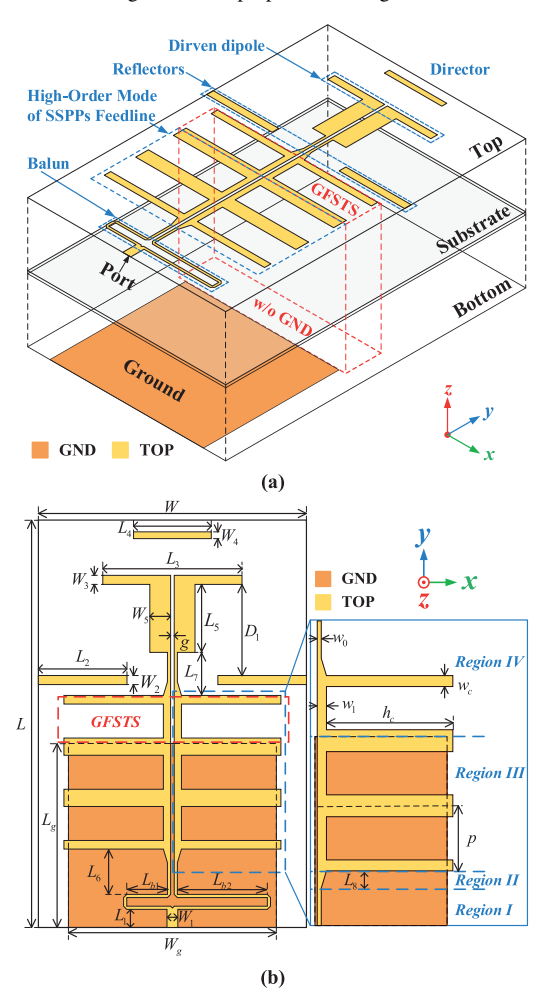


Fig. 2. Structure of the proposed high-gain wideband filtering quasi-Yagi antenna with high-order mode of SSPPs. (a) Perspective view. (b) Top view.

port is connected to a balun, enabling differential feeding for the driven dipole and resulting in the formation of RNs4 and RN6 in the lower and upper stopbands.

# III. DESIGN AND ANALYSIS OF FILTERING QUASI-YAGI ANTENNA WITH SSPP STRUCTURE

## A. Mechanism of Filtering Performance Based on High-Order Mode of SSPPs

The unit cell of the employed SSPP structure and its dispersion curve is illustrated in Fig. 3. The top and bottom layers of the Rogers 5880 substrate are patterned with U-shaped metallic strips and a ground plane, respectively. The thickness of the dielectric substrate is 0.787 mm. To minimize

Authorized licensed use limited to: TOHOKU UNIVERSITY. Downloaded on October 20,2025 at 02:20:52 UTC from IEEE Xplore. Restrictions apply.

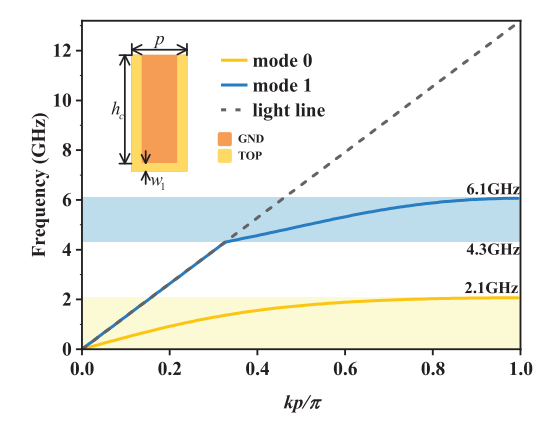


Fig. 3. Simulated dispersion curves for the first two modes of the U-shape unit in Fig. 2 ( $h_c = 22 \text{ mm}$ , p = 11.3 mm,  $w_c = 1.9 \text{ mm}$ , and  $w_1 = 1.6 \text{ mm}$ ).

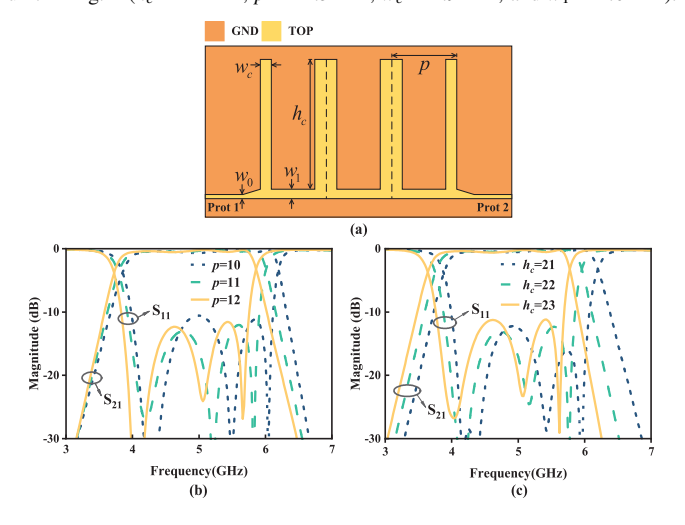


Fig. 4. (a) Configurations of bandpass filter based on mode 1 of the proposed U-shape unit and its simulated S-parameters against (b) parameter p and (c) parameter  $h_c$ .

the influence of material thickness on the simulation results, the thickness of the metallic layers is set to 0.035 mm. In order to excite the high-order mode of SSPPs of the U-shape unit, the depth of the groove  $h_c$  of the unit must be greater than the period p. The number of modes N for the SSPPs can be approximately expressed as

$$N = 1 + \operatorname{int}(h_c/p). \tag{1}$$

Numerical analysis of the unit's dispersion characteristics is performed using the eigenmode solver in CST Microwave Studio. In Fig. 3, the dispersion curves exhibit multiple branches across different frequency bands, demonstrating typical SPP-like behavior. As the frequency increases, both curves diverge from the light line in free space, entering the slow wave region, and reach a horizontal asymptotic frequency limit at the edge of the first Brillouin zone. This result indicates that the designed U-shape unit simultaneously supports both fundamental (mode 0) and high-order (mode 1) modes of SSPPs, which is consistent with the number of modes obtained from (1). These modes correspond to distinct frequency bands that are isolated from each other, allowing for the formation of a passband for single-mode transmission only.

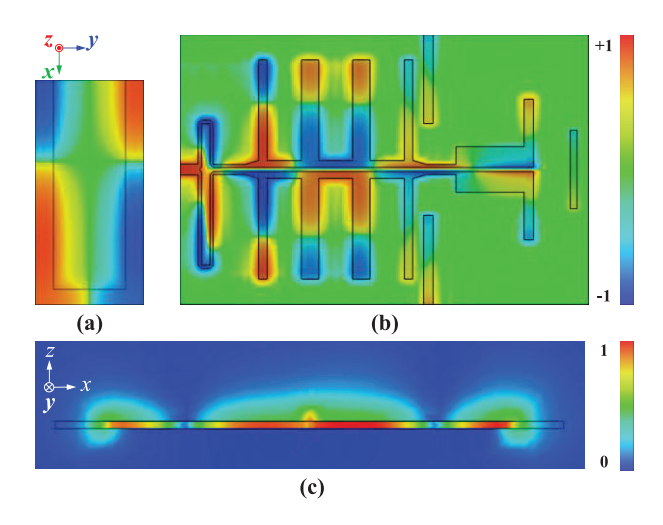


Fig. 5. Normalized z component of the electric field distributions of (a) mode 1 at asymptotic frequencies 6.1 GHz and (b) proposed filtering antenna at the frequencies of 5.8 GHz. (c) Normalized amplitude of electric field in the cross section perpendicular to the strip. The color bar indicates the electric field polarity and field strength on a logarithm scale.

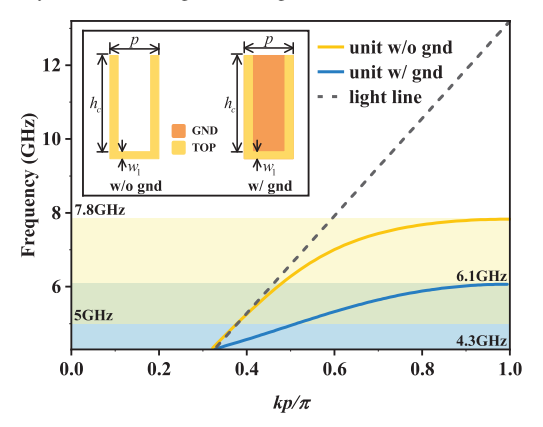


Fig. 6. Dispersion curves for mode 1 of the grounded U-shaped unit and the ground-free U-shaped unit.

As mentioned above, mode 1, which is isolated from mode 0, exhibits bandpass response characteristics. Therefore, no additional filtering structures are required, and the desired passband can be achieved by simply designing the geometry of the SSPPs unit, as shown in Fig. 4. A simple and compact trapezoidal structure enables smooth matching between the SSPPs waveguide operating in mode 1 and the microstrip line, as shown in region II of Fig. 2. However, since it cannot provide smooth matching for the SSPPs waveguide operating in mode 0, this transition structure effectively suppresses low-frequency signals from passing through the passband associated with mode 0, thereby enhancing the out-of-band rejection of the filtering antenna. Simulation results show that the in-band insertion loss is less than 0.5 dB, and the return loss is better than 10 dB. To further verify the proposed antenna's support for the high-order mode of SSPPs, the simulated electric field distribution of the proposed antenna at 5.8 GHz is illustrated in Fig. 5(b). As can be observed, the energy is efficiently transmitted to the driven dipole, and the feeding line supporting SSPPs shows an electric field distribution consistent with that of the U-shape unit in the

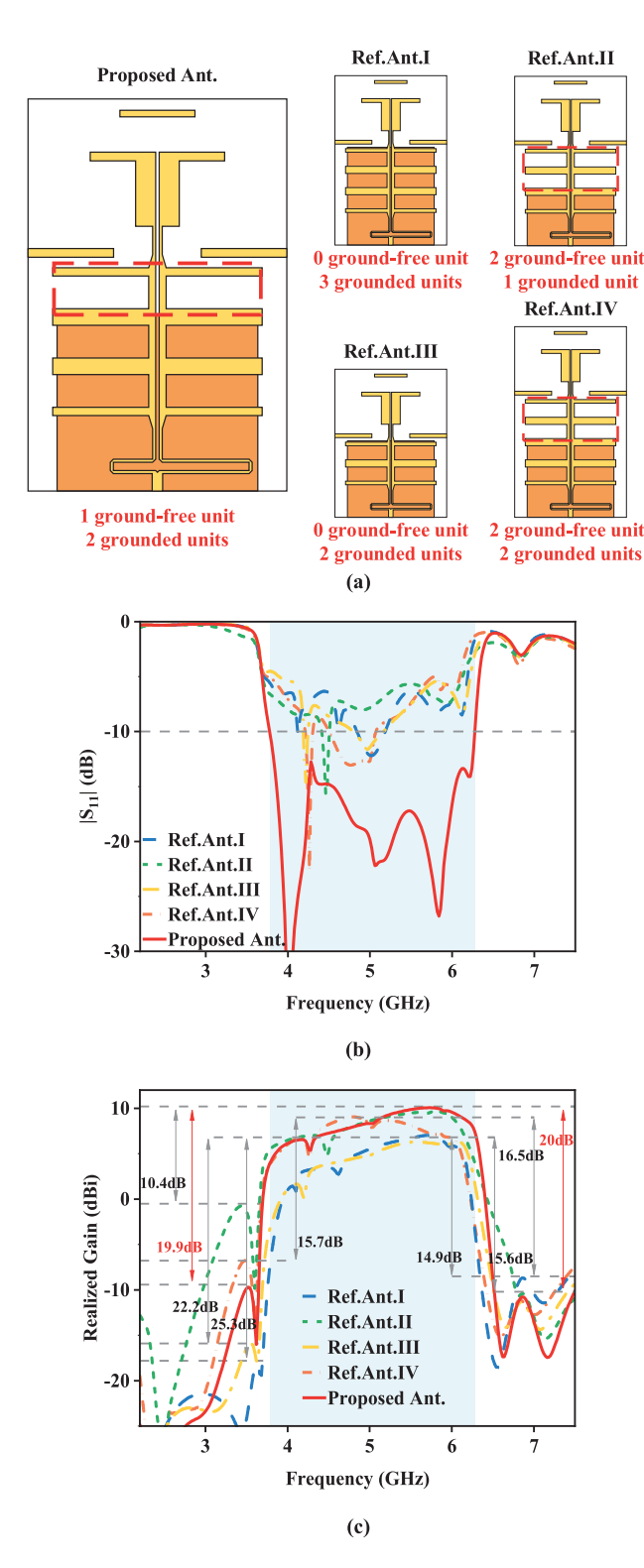
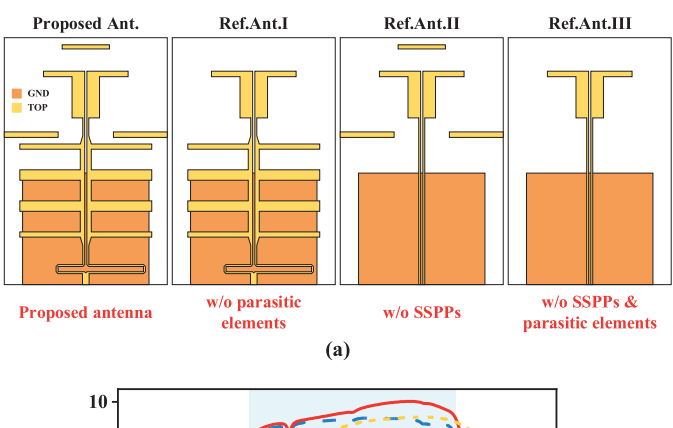


Fig. 7. (a) Configurations of the reference and proposed antennas and their corresponding performance, (b)  $|S_{11}|$ , and (c) realized gain.

mode 1 region, as shown in Fig. 5(a) and obtained from the eigenmode simulation. The proposed antenna exhibits similar typical electric field characteristics. The electromagnetic energy is tightly confined near the metallic strips, with the maximum of electric field magnitude symmetrically distributed along the geometric axis of the unit. Moreover, each metallic strip of the U-shaped unit can be divided into two distinct



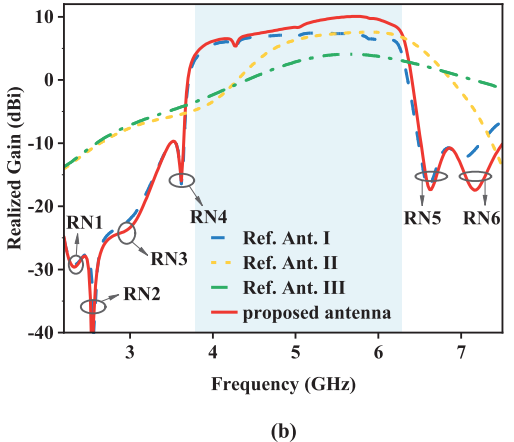


Fig. 8. (a) Configuration and (b) simulated results of realized gain with/without SSPP structure, reflectors, and director.

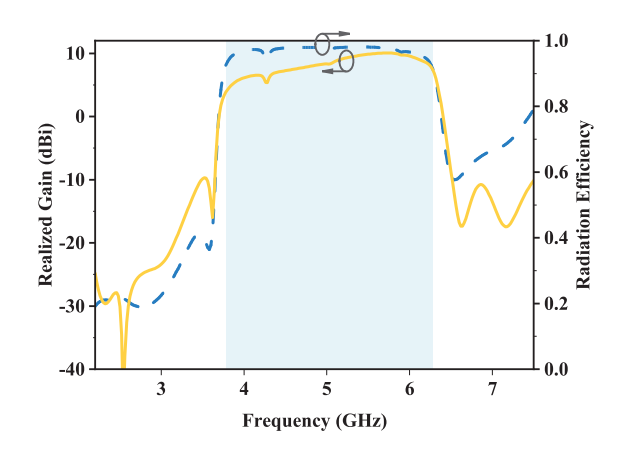


Fig. 9. Simulated result of realized gain and radiation efficiency of the proposed filtering antenna.

regions based on the direction of the z-component electric field distribution on its surface. From the side view in Fig. 5(c), a strong confinement effect is evident, demonstrating the characteristic binding of the field near the structure.

### B. Principle of GFSTS

As previously mentioned, the energy is tightly confined around the metallic strips, allowing only signals within the passband corresponding to mode 1 to propagate. However, it is challenging to directly feed energy from the SSPP

strips into the driven dipole. To address this issue, the novel GFSTS is proposed, enabling seamless momentum transition and impedance matching between the high-order mode of SSPP filtering structure and the driven dipole.

The dispersion curves for mode 1 of the grounded U-shaped unit and the ground-free U-shaped unit are shown in Fig. 6. The cutoff frequency of the ground-free U-shaped unit is higher than that of the grounded U-shaped unit, indicating relatively weaker electromagnetic confinement in the groundfree unit. Additionally, the propagation wavenumber in the y-direction for the ground-free U-shaped unit falls between that of the grounded U-shaped unit and the light line. The GFSTS, employing a ground-free U-shaped unit to bridge the SSPP feedline and the driven dipole, facilitates a smooth momentum transition. This structure enables the propagating SPP waves to be effectively converted into guided waves, in contrast to a direct transition to the driven dipole. As a result, energy is efficiently fed into the driven dipole while maintaining the filtering characteristics of the high-order mode of SSPPs.

However, to achieve broadband filtering characteristics, ensure efficient transition from the SSPP structure to the driven dipole, and maintain compact antenna dimensions, the proposed novel transition structure is designed with a single ground-free U-shaped unit. Fig. 7 illustrates the relationship between the number of ground-free U-shaped units in the transition structure and the antenna performance. Compared to the reference antenna, the antenna with a single-unit transition structure shows superior performance in terms of realized gain in the endfire direction (+y axis), return loss, and out-of-band suppression, confirming the necessity of the single-unit design.

#### C. High-Gain Characteristics of the Antenna

The quasi-Yagi antenna design has been employed to achieve endfire radiation. The integration of the high-order mode of SSPPs with the quasi-Yagi antenna ultimately achieves high-gain and broadband characteristics. As shown in the gain comparison curve in Fig. 8, the reflector, director, and ground reflection effectively enhance the antenna's aperture, resulting in a significant gain improvement compared to a standard dipole antenna. Additionally, the configuration of the reflector and its relative position to the SSPPs provides excellent directivity for the antenna.

The feed line supporting the high-order mode of SSPPs exhibits relatively lower transmission loss, which improves the antenna's radiation efficiency and enhances its gain. According to the perturbation theory, the attenuation constant of a microwave transmission line can be expressed as

$$\alpha \approx \frac{\omega_0 \varepsilon \tan \delta \iint_{\Delta S} \left| \overrightarrow{E_0} \right|^2 dS}{\iint_{S} \left( \overrightarrow{E_0}^* \times \overrightarrow{H_0} + \overrightarrow{H_0}^* \times \overrightarrow{E_0} \right) \cdot dS}$$
 (2)

where  $\Delta S$  and S represent the areas of the substrate and total space, respectively, and the denominator represents twice the mean power flow of the transmission line. It can be observed that for transmission lines with equal power transmission, the attenuation constant  $\alpha$  is positively correlated with the distribution of electric field energy within the substrate. From the

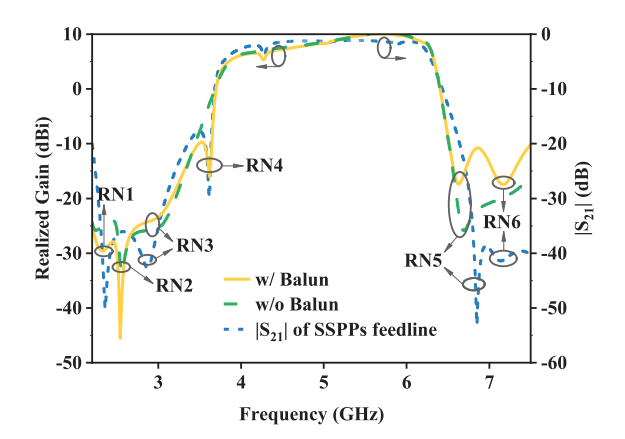


Fig. 10. Simulated result of realized gain with/without balun and |S21| of SSPP feeding line.

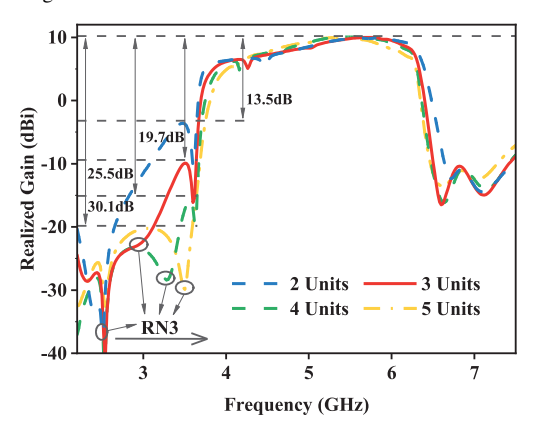


Fig. 11. Simulated result of realized gain of the proposed antenna with different total numbers of U-shape units.

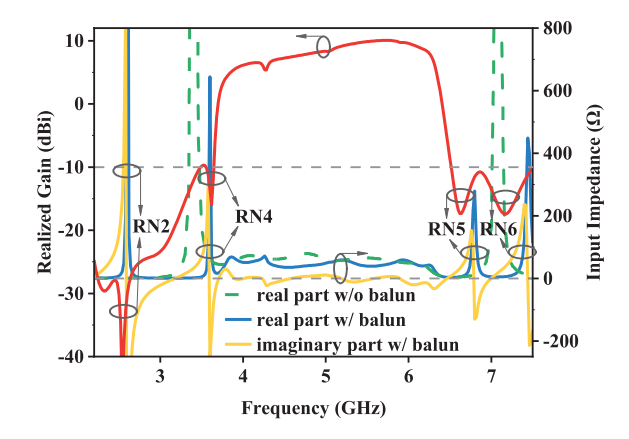


Fig. 12. Realized gain of the proposed antenna and input impedance with/without balun.

electric field distribution characteristics in Fig. 5(c), compared to traditional structures, such as microstrip lines, there are more electromagnetic fields confined to the air around SSPPs, while the electromagnetic fields distributed in the dielectric substrate are correspondingly weaker. Therefore, according to (2), the SSPP feedline employed in the proposed antenna exhibits lower transmission loss.

Therefore, due to the unique electric field distribution characteristics of the SSPP structure, the SSPP feedline used

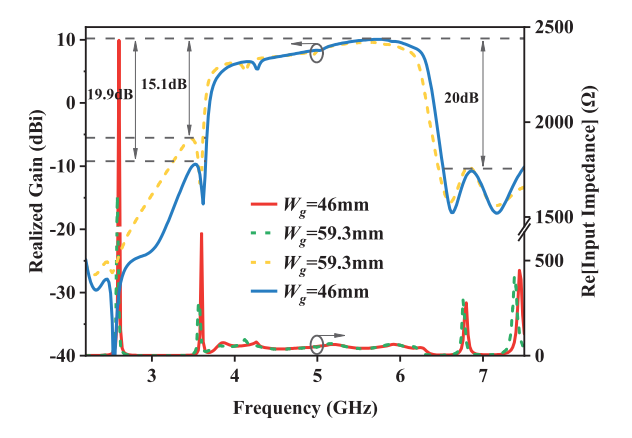


Fig. 13. Realized gain and real part of input impedance of the proposed antenna against parameter  $W_g$ .

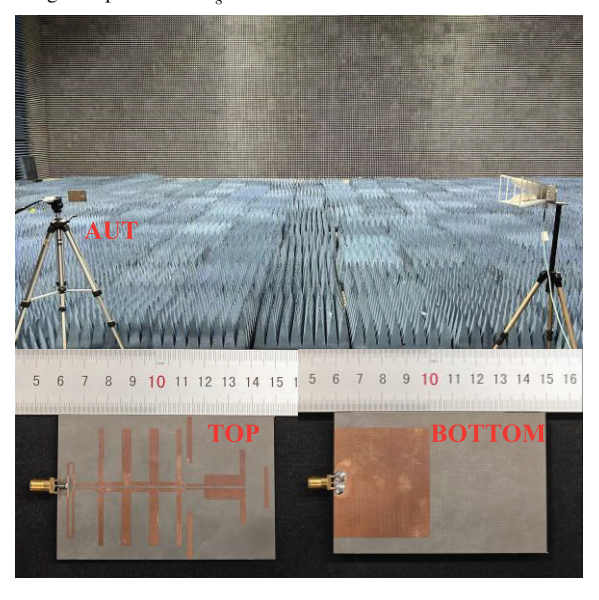


Fig. 14. Photograph of fabricated high-gain wideband quasi-Yagi filtering antenna based on high-order mode of SSPPs.

in this work exhibits inherently lower loss, enabling higher transmission efficiency. Additionally, the single-mode transmission characteristics of the high-order mode of SSPPs can independently achieve the antenna's filtering function without requiring additional filtering structures, which may otherwise reduce radiation efficiency. This approach further enhances the overall radiation efficiency. Through comparative simulations, the gain curve shown in Fig. 9 demonstrates that the antenna achieves not only filtering characteristics but also a significant gain enhancement, with a simulated peak gain reaching 10.1 dBi and the simulated in-band radiation efficiency over 94%.

#### D. Mechanism of the RNs

As shown in Fig. 8, RN1–RN6 are introduced in the stopbands by the proposed antenna. The following analysis will investigate the mechanisms behind the generation of these RNs. The antenna feed line operates in the high-order mode of SSPPs, introducing natural stopbands that arise from the interactions between different modes of the SSPPs. This results in the formation of three RNs located at 2.32, 2.54,

and 6.64 GHz, respectively, namely RN1, RN2, and RN5, corresponding to the transmission coefficient curve of the SSPP feed structure in Fig. 10. The depression in the radiation pattern of the proposed antenna at 2.96 GHz in the endfire direction has led to the formation of a spatial RN, labeled as RN3. It is noteworthy that within a certain range, the more units the SSPP feedline consists of, the better the roll-off of the stopband will be. As shown in Fig. 11, with the increase in the number of units, RN3 shifts toward higher frequencies, thereby improving the frequency selectivity of the antenna. To balance the antenna's performance and profile, the proposed high-gain filtering quasi-Yagi antenna employs a design with three units. Additionally, the new resonance modes generated by the metallic strips broaden the bandwidth of the proposed antenna.

To facilitate feeding, a balun is designed as shown in Fig. 2(b) to excite the dipole for radiating electromagnetic waves. As shown in Fig. 12, after the introduction of the balun, the real part of the antenna's input impedance significantly increases at 3.6 and 7.4 GHz, preventing efficient energy transfer to the radiating elements and thus generating RNs4 and RN6, which improves the roll-off of the stopband of the proposed antenna. The introduction of the balun causes the proposed antenna to further severely mismatch at RN2, increasing the depth of RN2. Additionally, the impedance peak at 7.1 GHz shifts slightly toward the lower frequencies and decreases, which reduces the depth of RN5, as illustrated in Fig. 10. However, a minor peak appears at 4.2 GHz on the real part of the input impedance curve, causing a slight suppression in antenna gain. The use of the balun not only simplifies testing but also improves the roll-off rate of the lower stopband, enhancing the antenna's frequency selectivity.

Additionally, reducing the ground width  $W_g$ , as shown in Fig. 2(b), increases the real part of the input impedance of the proposed antenna from 1500 to 2500  $\Omega$ , which improves the depth of RN2 from -26 to -45 dBi, thereby effectively enhancing the suppression of the lower stopband, as shown in Fig. 13.

#### IV. FABRICATION AND MEASUREMENT RESULTS

To verify the feasibility of the design, a prototype of the proposed high-gain wideband filtering quasi-Yagi antenna based on the high-order mode of SSPPs is fabricated and measured. The final parameters of the proposed high-gain wideband filtering quasi-Yagi antenna based on the high-order mode of SSPPs are as follows: L = 89.9 mm,  $L_1 = 4$  mm,  $L_2 = 19.6$  mm,  $L_3 = 30.8$  mm,  $L_4 = 17.2$  mm,  $L_5 = 15$  mm,  $L_6 = 10$  mm,  $L_7 = 9.5$  mm,  $L_8 = 3$  mm,  $L_{b1} = 9$  mm,  $L_{b2} = 19.9$  mm,  $L_g = 40.6$  mm, W = 59.3 mm,  $W_g = 46$  mm,  $W_1 = 2.4$  mm,  $W_2 = 2$  mm,  $W_3 = 2$  mm,  $W_4 = 1.5$  mm,  $W_5 = 4.6$  mm,  $D_1 = 20.1$  mm,  $W_0 = 0.7$  mm,  $W_1 = 1.6$  mm,  $W_2 = 1.9$  mm,  $W_3 = 2$  mm, and  $W_3 = 11.3$  mm.

The photograph of the proposed high-gain wideband filtering quasi-Yagi antenna based on the high-order mode of SSPPs is shown in Fig. 14. Considering the practical requirements in communication systems, Fig. 15 illustrates the radiation patterns of the proposed antenna in the E (XOY) and H (YOZ)

P.G. R.O.R. Sup. Ref. **FBW** Nulls Size( $\lambda_0^3$ ) Filtering Design Method (dBi) (dB) (dB/GHz) [1] 18.5% 5.8 2 10/15 16/42  $0.76 \times 0.44 \times 0.01$ Stub-loaded resonator Exponential curved branch [2] 85.1% 8.3 6 14/17 16/12  $0.49 \times 0.35 \times 0.01$ + Parasitic elements [7] 50% 8.1 3 30/16 51/40  $1.03 \times 1.03 \times 0.24$ Balun feed  $2.652 \times 0.980 \times$ Fundamental mode of [20] 10 0 12/12 1.4/12 57.1% **SSPPs** 0.035 Fundamental mode of  $4.344 \times 1.529 \times$ 10.44% 9.38 2 SSPPs+ Via holes + Ring [24] 26/17 21/72 0.03 resonators  $1.507 \times 0.994 \times$ This High-order Mode of 50.5% 9.98 6 21/19 92/58 **SSPPs** work 0.013

 ${\bf TABLE~I}$  Comparison of the Proposed Antenna with Some Existing Works

Ref.: Reference, P.G.: Peak Gain, Sup.: Suppression, R.O.R.: Roll-off Rate

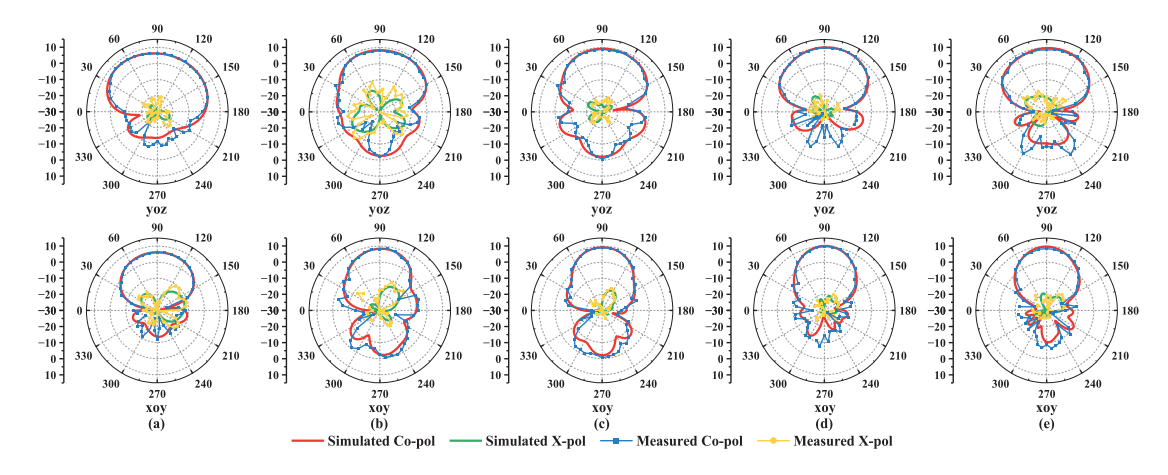


Fig. 15. Measured and simulated radiation patterns of the proposed filtering quasi-Yagi antenna prototype at (a) 4, (b) 5, (c) 5.2, (d) 5.8, and (e) 6 GHz.

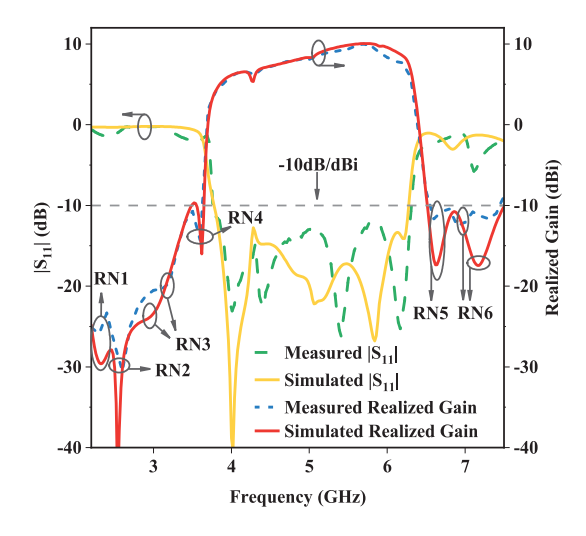


Fig. 16. Measured and simulated results of the proposed high-gain wideband filtering quasi-Yagi antenna based on high-order mode of SSPPs.

planes at frequencies of 4, 5, 5.2, 5.8, and 6 GHz. The results demonstrate good endfire characteristics with well-suppressed sidelobes. Across the entire passband, the measured

cross-polarization levels in the E- and H-planes are below -16.4 and -15 dB, respectively. The measured and simulated S-parameters and realized gains are presented in Fig. 16. The measurement results indicate that the reflection coefficient  $|S_{11}|$  is below -10 dB within the range of 3.76–6.3 GHz, achieving a fractional bandwidth (FBW) of 50.5%, which closely aligns with the simulation. The measured peak gain within the passband is 9.98 dBi at 5.7 GHz. Additionally, the antenna achieves 18.8-dB out-of-band suppression. To further highlight the advantages of the proposed antenna, a performance comparison with previously reported antennas of similar types in terms of gain, bandwidth, and out-of-band suppression is presented in Table I. It can be observed that the proposed quasi-Yagi antenna based on the high-order mode of SSPPs features a simple structure, wide bandwidth, excellent out-of-band suppression, and high gain.

#### V. CONCLUSION

In this article, a high-gain, wideband filtering antenna based on the high-order mode of SSPPs is proposed. By adjusting the geometry of the metallic strips, a feedline operating in the high-order mode of SSPPs with single-mode transmission characteristics is achieved in the target frequency band. Combined with a specially designed balun and ground plane, excellent filtering characteristics with six RNs are obtained. The novel GFSTS, serving as a compact alternative to traditional tapered transitions, facilitates momentum transition and impedance matching between the SSPP feedline and the driven dipole, ensuring efficient energy transfer. Leveraging the low-loss characteristics of the SSPP feedline, this design avoids the insertion loss typical of traditional filtering structures, enhancing radiation efficiency while providing the filtering function of a quasi-Yagi antenna. The measured peak gain reaches 9.98 dBi, with the antenna demonstrating excellent endfire radiation characteristics. The proposed antenna is fabricated and measured, and the measured and simulated results agree well.

#### REFERENCES

- [1] F. Wei, X.-B. Zhao, and X. W. Shi, "A balanced filtering quasi-Yagi antenna with low cross-polarization levels and high common-mode suppression," *IEEE Access*, vol. 7, pp. 100113–100119, 2019, doi: 10.1109/ACCESS.2019.2931141.
- [2] D. Li, C. Yang, Y. Liu, L. Yang, and Q. Chen, "Planar printed wideband filtering quasi-Yagi antenna and its notch-band design using parasitic elements for vehicular communication," *IEEE Trans. Veh. Technol.*, vol. 73, no. 2, pp. 2122–2131, Feb. 2024, doi: 10.1109/TVT.2023.3314974.
- [3] D. Li, C. Yang, L. Shi, Y. Liu, Q. Chen, and N. Shinohara, "A high-gain filtering quasi-Yagi antenna based on compressed third-order mode dipole," *IEEE Antennas Wireless Propag. Lett.*, vol. 23, pp. 2860–2864, 2024, doi: 10.1109/LAWP.2024.3409748.
- [4] J. Deng, S. Hou, L. Zhao, and L. Guo, "Wideband-to-narrowband tunable monopole antenna with integrated bandpass filters for UWB/WLAN applications," *IEEE Antennas Wireless Propag. Lett.*, vol. 16, pp. 2734–2737, 2017, doi: 10.1109/LAWP.2017.2743258.
- [5] R. Hou, J. Ren, Y.-T. Liu, Y.-M. Cai, J. Wang, and Y. Yin, "Broadband magnetoelectric dipole filtering antenna for 5G application," *IEEE Antennas Wireless Propag. Lett.*, vol. 22, no. 3, pp. 497–501, Mar. 2023, doi: 10.1109/LAWP.2022.3216688.
- [6] X. Liu, K. W. Leung, and N. Yang, "Frequency reconfigurable filtering dielectric resonator antenna with harmonics suppression," *IEEE Trans. Antennas Propag.*, vol. 69, no. 6, pp. 3224–3233, Jun. 2021, doi: 10.1109/TAP.2020.3044387
- [7] S. J. Yang, Y. F. Cao, Y. M. Pan, Y. Wu, H. Hu, and X. Y. Zhang, "Balun-fed dual-polarized broadband filtering antenna without extra filtering structure," *IEEE Antennas Wireless Propag. Lett.*, vol. 19, no. 4, pp. 656–660, Apr. 2020, doi: 10.1109/LAWP.2020.2975844.
- [8] C. Feng Ding, X. Yin Zhang, and M. Yu, "Simple dual-polarized filtering antenna with enhanced bandwidth for base station applications," *IEEE Trans. Antennas Propag.*, vol. 68, no. 6, pp. 4354–4361, Jun. 2020, doi: 10.1109/TAP.2020.2975282.
- [9] Q. Liu and L. Zhu, "A compact wideband filtering antenna on slots-loaded square patch radiator under triple resonant modes," *IEEE Trans. Antennas Propag.*, vol. 70, no. 10, pp. 9882–9887, Oct. 2022, doi: 10.1109/TAP.2022.3184494.
- [10] W. Yang et al., "A simple, compact filtering patch antenna based on mode analysis with wide out-of-band suppression," *IEEE Trans. Antennas Propag.*, vol. 67, no. 10, pp. 6244–6253, Oct. 2019, doi: 10.1109/TAP.2019.2922770.
- [11] N.-W. Liu, Y.-D. Liang, L. Zhu, Z.-X. Liu, and G. Fu, "A low-profile, wideband, filtering-response, omnidirectional dielectric resonator antenna without enlarged size and extra feeding circuit," *IEEE Antennas Wireless Propag. Lett.*, vol. 20, no. 7, pp. 1120–1124, Jul. 2021, doi: 10.1109/LAWP.2021.3072062.
- [12] W. Yang, M. Xun, W. Che, W. Feng, Y. Zhang, and Q. Xue, "Novel compact high-gain differential-fed dual-polarized filtering patch antenna," *IEEE Trans. Antennas Propag.*, vol. 67, no. 12, pp. 7261–7271, Dec. 2019, doi: 10.1109/TAP.2019.2930213.
- [13] J.-Y. Lin, Y. Yang, S.-W. Wong, and Y. Li, "High-order modes analysis and its applications to dual-band dual-polarized filtering cavity slot arrays," *IEEE Trans. Microw. Theory Techn.*, vol. 69, no. 6, pp. 3084–3092, Jun. 2021, doi: 10.1109/TMTT.2021.3072945.
- [14] R. Lu et al., "SIW cavity-fed filtennas for 5G millimeter-wave applications," *IEEE Trans. Antennas Propag.*, vol. 69, no. 9, pp. 5269–5277, Sep. 2021, doi: 10.1109/TAP.2021.3061110.

- [15] J. Qian, F. Chen, Y. Ding, H. Hu, and Q. Chu, "A wide stopband filtering patch antenna and its application in MIMO system," *IEEE Trans. Antennas Propag.*, vol. 67, no. 1, pp. 654–658, Jan. 2019, doi: 10.1109/TAP.2018.2874764.
- [16] X. Gao et al., "Ultra-wideband surface plasmonic Y-splitter," Opt. Exp., vol. 23, no. 18, p. 23270, Sep. 2015, doi: 10.1364/oe.23.023270.
- [17] Q. L. Zhang and C. H. Chan, "Compact spoof surface plasmon polaritons waveguide integrated with blind vias and its applications," *IEEE Trans. Circuits Syst. II, Exp. Briefs*, vol. 67, no. 12, pp. 3038–3042, Dec. 2020, doi: 10.1109/TCSII.2020.3001297.
- [18] C. H. Wang, X. M. Shi, H. L. Yang, and X. L. Xi, "A flexible amplitude equalizing filter based on spoof surface plasmon polaritons," *IEEE Trans. Antennas Propag.*, vol. 71, no. 7, pp. 5777–5785, Jul. 2023, doi: 10.1109/TAP.2023.3266864.
- [19] X. Du, H. Li, and Y. Yin, "Wideband fish-bone antenna utilizing odd-mode spoof surface plasmon polaritons for endfire radiation," *IEEE Trans. Antennas Propag.*, vol. 67, no. 7, pp. 4848–4853, Jul. 2019, doi: 10.1109/TAP.2019.2913707.
- [20] H. Qi and H. Liu, "Wideband high-gain filtering Vivaldi antenna design based on MS and herringbone SSPP structure," *IEEE Antennas Wireless Propag. Lett.*, vol. 22, no. 8, pp. 1798–1802, Aug. 2023, doi: 10.1109/ LAWP.2023.3264702.
- [21] Z. Lin, Y. Li, L. Li, Y. Zhao, J. Xu, and J. Chen, "Miniaturized bandpass filter based on high-order mode of spoof surface plasmon polaritons loaded with capacitor," *IEEE Trans. Plasma Sci.*, vol. 51, no. 1, pp. 254–260, Jan. 2023, doi: 10.1109/TPS.2022.3232850.
- [22] K.-D. Xu, S. Lu, Y.-J. Guo, and Q. Chen, "High-order mode of spoof surface plasmon polaritons and its application in bandpass filters," *IEEE Trans. Plasma Sci.*, vol. 49, no. 1, pp. 269–275, Jan. 2021, doi: 10.1109/ TPS.2020.3043889.
- [23] Z. Liang, S.-S. Qi, and W. Wu, "Ultra-wideband planar end-fire antenna based on high-order modes of spoof surface plasmon polaritons," *IEEE Trans. Antennas Propag.*, vol. 71, no. 2, pp. 1469–1477, Feb. 2023, doi: 10.1109/TAP.2022.3227750.
- [24] W. Feng, Y. Feng, W. Yang, W. Che, and Q. Xue, "High-performance filtering antenna using spoof surface plasmon polaritons," *IEEE Trans. Plasma Sci.*, vol. 47, no. 6, pp. 2832–2837, Jun. 2019, doi: 10.1109/ TPS.2019.2915627.
- [25] A. Kandwal, Q. Zhang, X.-L. Tang, L. W. Liu, and G. Zhang, "Low-profile spoof surface plasmon polaritons traveling-wave antenna for near-endfire radiation," *IEEE Antennas Wireless Propag. Lett.*, vol. 17, pp. 184–187, 2018, doi: 10.1109/LAWP.2017.2779455.



**Daotong Li** (Senior Member, IEEE) received the Ph.D. degree in electromagnetic field and microwave technology from the University of Electronic Science and Technology of China, Chengdu, China, in 2016

He has been a Visiting Researcher with the Department of Electrical and Computer Engineering, University of Illinois at Urbana–Champaign, Champaign, IL, USA, from 2015 to 2016, later joining Chongqing University as an Assistant Professor in 2017 and being promoted to Associate Professor in

2019. His academic journey includes being awarded a JSPS Fellowship at Tohoku University from November 2021 to 2023, as a Visiting Associate Professor at Kyoto University, Kyoto, Japan, in 2024, and has been a Guest Scholar since June 2024. He is currently with the Center of Tracking Telemetry Command, Chongqing University, Chongqing. His research focuses on RF/microwave/millimeter-wave technologies, microwave power transmission (MPT), and antennas, with over 100 peer-reviewed publications.

Dr. Li's achievements include receiving the UESTC Outstanding Graduate Awards in 2016, the National Graduate Student Scholarship, and the "Tang Lixin" Scholarship. His professional service includes reviewing for IEEE/IET journals and participating in international conferences as a TPC member, a session organizer, and the chair.



Ning Pan received the B.S. degree from Yantai University, Yantai, China, in 2023. He is currently pursuing the M.S. degree in information and communication engineering with the School of Microelectronics and Communication Engineering, Chongqing University, Chongqing, China.

His current research interests include filtering antennas, surface plasmonic polariton (SPP) devices, and filters.



**Ying Liu** received the M.S. degree in communication and information system from Chongqing University, Chongqing, China, in 2015.

She is currently with the College of Microelectronics and Communication Engineering, Chongqing University. Her research focuses on microwave photonics and image processing.



Hao Wang received the B.S. degree from South-Central Minzu University, Wuhan, China, in 2023. He is currently pursuing the M.S. degree in electronic information with the School of Microelectronics and Communication Engineering, Chongqing University, Chongqing, China.

His current research interests include microwave circuits and systems.



Jiang Dong (Graduate Student Member, IEEE) received the B.S. degree from Chengdu University of Technology, Chengdu, China, in 2022. He is currently pursuing the M.S. degree in information and communication engineering with the School of Microelectronics and Communication Engineering, Chongqing University, Chongqing, China.

His current research interests include microwave power transmission, slot antennas, and array antennas.



**Qi Jiang** received the B.S. degree from Henan University, Kaifeng, China, in 2023. He is currently pursuing the M.S. degree in information and communication engineering with the School of Microelectronics and Communication Engineering, Chongqing University, Chongqing, China.

His current research interests include filters, nonreciprocity, and substrate integrated waveguide devices.



Naoki Shinohara (Fellow, IEEE) received the Ph.D. degree in electrical engineering from Kyoto University, Kyoto, Japan, in 1996.

He has been affiliated with Kyoto University since 1996, becoming a Professor in 2010, where he conducts pioneering research on solar power satellites and microwave power transmission systems. He is currently a Professor with the Research Institute for Sustainable Humanosphere, Kyoto University. He has authored seminal works, including *Wireless Power Transfer via Radiowaves* (Wiley, 2014), and

edited several authoritative volumes on wireless power technologies.

Dr. Shinohara was a current IEEE AdCom Member from 2022 to 2024. He plays multiple leadership roles across prestigious organizations: he founded the IEEE Wireless Power Transfer Conference and serves on its Steering Committee, chairs URSI Commission D and the Wireless Power Transfer Consortium for Practical Applications (WiPoT), acts as an Executive Editor for *International Journal of Wireless Power Transfer*, and holds the Vice-Chairmanship of the Space Solar Power Systems Society. His extensive committee engagements span IEEE MTT-S Technical Committee 25, IEICE Wireless Power Transfer, and various Japanese research consortia, cementing his status as a global leader in advancing wireless power technologies. He was an IEEE Distinguished Microwave Lecturer from 2016 to 2018.



Qiang Chen (Senior Member, IEEE) received the B.E. degree from Xidian University, Xi'an, China, in 1986, and the M.E. and D.E. degrees from Tohoku University, Sendai, Japan, in 1991 and 1994, respectively.

He is currently a Chair Professor with the Electromagnetic Engineering Laboratory, Department of Communications Engineering, Faculty of Engineering, Tohoku University. His primary research interests include antennas, microwave and millimeter wave, electromagnetic measurement, and computa-

tional electromagnetics.

Dr. Chen is an IEICE Fellow. He received the Best Paper Award and Zenichi Kiyasu Award from the Institute of Electronics, Information and Communication Engineers (IEICE). He served as the Chair for the IEICE Technical Committee on Photonics-Applied Electromagnetic Measurement from 2012 to 2014, the IEICE Technical Committee on Wireless Power Transfer from 2016 to 2018, the IEEE Antennas and Propagation Society Tokyo Chapter from 2017 to 2018, and the IEICE Technical Committee on Antennas and Propagation from 2019 to 2021.